

C-WSL: Count-guided Weakly Supervised Localization

Mingfei Gao, Ang Li*, Ruichi Yu, Vlad I. Morariu, Larry S. Davis

University of Maryland, College Park, MD, 20742

{mgao, angli, richyu, morariu, lsd}@umiacs.umd.edu

Abstract

We introduce a count-guided weakly supervised localization (C-WSL) framework with per-class object count as an additional form of image-level supervision to improve weakly supervised localization (WSL). C-WSL uses a simple count-based region selection algorithm to select high-quality regions, each of which covers a single object instance at training time, and improves WSL by training with the selected regions. To demonstrate the effectiveness of C-WSL, we integrate object count supervision into two WSL architectures and conduct extensive experiments on Pascal VOC2007 and VOC2012. Experimental results show that C-WSL leads to large improvements in WSL detection performance and that the proposed approach significantly outperforms the state-of-the-art methods.

1. Introduction

Convolutional neural networks (CNN) have achieved state-of-the-art performance on the object detection task, *e.g.*, Faster-RCNN [25], SSD [19], YOLO [23, 24]. However, these detectors are trained in a strongly supervised setting, requiring large amounts of bounding box annotations and huge amounts of human labor.

To ease the burden of human annotation, weakly supervised localization (WSL) methods train a detector using weak supervision, *e.g.*, image-level supervision, instead of tight object bounding boxes. The presence of an object category in an image can be obtained on the Internet nearly for free, so most existing WSL architectures require only object categories as supervision.

Existing methods [1, 3, 5, 14, 20, 30, 29, 17, 13, 31, 15, 26, 28] have proposed different architectures to address the WSL problem. However, there is still a large performance gap between weakly and strongly supervised detectors [25, 24, 19] on standard object detection benchmarks [10, 11, 18]. Often, this is because the limited in-

*Now at Google DeepMind

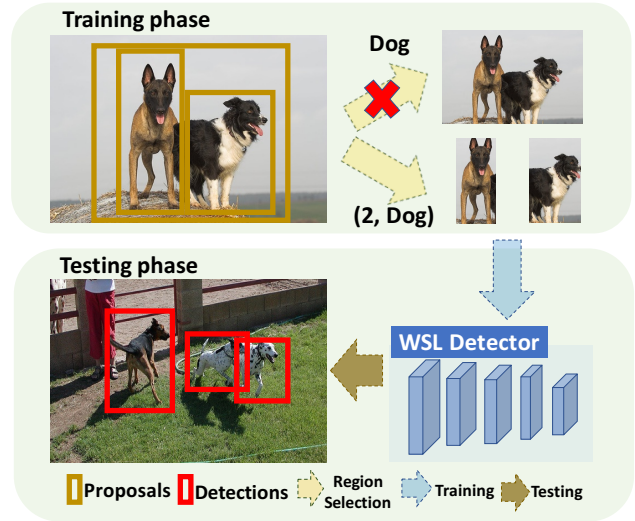


Figure 1. Given a set of object proposals and the per-class object count label, we select high-quality positive regions (that tightly cover a single object) to train a WSL detector. Count information significantly reduces detected bounding boxes that are loose and contain two or more object instances, one of the most common errors produced by weakly supervised detectors.

formation provided by object-category supervision. One major unsolved problem of WSL is that high confidence detections produced by the existing WSL detectors tend to include multiple objects instead of one. As shown in Fig. 1 (red cross branch), since training images with multiple dogs are labeled just as "Dog", detectors will learn the appearance of multiple dogs as if they were one dog and group multiple dogs as a single instance at test time. To resolve this ambiguity, we propose to use per-class object count information in images to supervise detector training. Object count is a much weaker and cheaper image-level supervision than instance-level supervisions, such as the bounding boxes. Unlike the bounding box annotation which requires several well-trained annotators to specify tight boxes on each object, object count can be obtained

without actually clicking on an object. Moreover, a widely studied phenomenon in psychology, called subitizing [4], suggests that humans are able to determine the number of objects without pointing or fixating on each object sequentially if the total number of objects in the image is small (typically 1-4) [2]. Thus, people may be able to specify the object count with just a glance.

Our proposed method, Count-guided WSL (C-WSL), is illustrated in Fig. 1. During the training process, C-WSL makes use of per-class object count supervision to identify the correct high-scoring object bounding boxes from a set of object proposals. Then, a weakly supervised detector is refined with these high-quality regions as pseudo ground-truth (GT) bounding boxes. This strategy is similar to existing WSL methods that refine detectors using automatically identified bounding boxes [17, 13, 29]. However, since these methods do not make use of object count supervision, they treat only the top-scoring region as the pseudo GT box, regardless of the number of object instances present in the image. This sometimes leads to multiple object instances being grouped into a single pseudo GT box, which hurts the detector’s ability to localize individual objects. With the guidance of the object count label, C-WSL selects tight box regions that cover individual objects as shown in Fig. 1 (the “(2, Dog)” branch).

The main contribution of C-WSL is that it uses per-class object count, a cheap and effective form of image-level supervision, to address a common failure case in WSL where one detected bounding box contains multiple object instances. To implement C-WSL, we develop a simple Count-based Region Selection (CRS) algorithm and integrate it into two existing architectures—alternating detector refinement (ADR) and online detector refinement (ODR)—to significantly improve WSL. Experimental results on Pascal VOC2007 [10] and VOC2012 [11] show that C-WSL significantly improves WSL detection and outperforms the state-of-the-art methods.

2. Related Works

MIL based CNN Methods. Most existing WSL methods [1, 3, 5, 14, 20, 30, 29, 17, 13] are based on multiple instance learning (MIL) [6]. In the MIL setting, a bag is defined as a collection of regions within an image. A bag is labeled as positive if at least one instance in the bag is positive and labeled as negative if all of its samples are negative. Under this assumption, the object location is obtained by identifying the positive region given image (bag) labels.

Bilen *et al.* [1] proposed a two-stream CNN architecture to classify and localize simultaneously and train the network in an end-to-end manner. Following [1], Kantorov *et al.* [14] added *additive* and *contrastive* models to improve localization on object boundaries instead of local parts. To avoid localizing on discriminative parts, Singh *et*

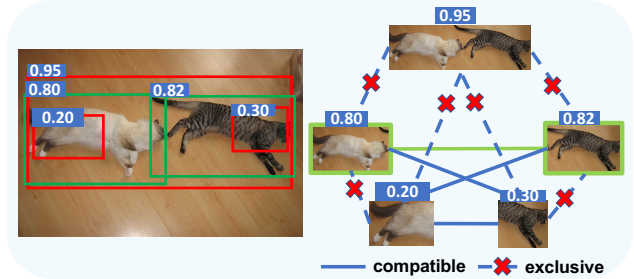


Figure 2. A common failure case of WSL methods (left) and graph representation of our region selection formulation (right). Our goal is to select the two green boxes, each of which tightly covers one object of interest, as the positive training samples for WSL detectors. We achieve this by analyzing the confidence score of each region and spatial constraints among regions.

al. [28] proposed ‘Hide-and-Seek’ framework which gradually hides patches to force WSL to consider different parts. In [17], Li *et al.* conducted progressive domain adaption and significantly improved the localization ability of the baseline detector. Diba *et al.* [5] performed WSL in two/three cascaded stages to find the best candidate location based on a generated class activation map. Jie *et al.* proposed a self-taught learning approach in [13] which alternates between classifier training and online supportive sample harvesting. Similarly, in [29], Tang *et al.* designed an online classifier refinement pipeline to progressively locate the most discriminative region of an image. These two works are most related to our approach since we also conduct alternating and online detector refinement. However, instead of using the top-scoring detection as the positive label [29] or mining confident regions by solving a complex dense subgraph discovery problem, we use per-class object count, a cheap form of supervision, to guide region selection and progressively obtain better positive training regions.

WSL with Additional Supervision. [21] proposed an efficient framework where an annotator verifies predicted results instead of manually drawing boxes. Kolesnikov *et al.* [16] assigned object or distractor labels to co-occurring objects in images to improve WSL. Papadopoulos *et al.* [22] proposed click supervision in WSL and integrated it into existing MIL based methods to improve localization performance. However, these methods either require frequent interactions with annotators or require annotators to search for and click on each instance in an image. In contrast, object count is an image-level annotation which contains less information (no location information at all). It can be obtained with no clicks and few interactions.

3. Proposed Approach

C-WSL selects regions covering a single object with the help of per-class object count supervision and then refines the WSL detector using these regions as the pseudo GT

bounding boxes. We first introduce a simple Count-based Region Selection (CRS) algorithm that C-WSL relies on to select high-quality regions from object proposals on training images. Then, we integrate CRS into two detector refinement structures to improve weakly supervised detectors.

3.1. Count-based Region Selection (CRS)

As shown in Fig. 2 (left), without object count information, previous methods often select the top-scoring box in training images as the positive training sample to refine the WSL detector [29, 17, 13]. Their detection performance is degraded because in many cases the top-scoring box contains multiple objects from the same category, *e.g.* two cats. Our goal is to select distinct regions, each covering single object (the two green boxes) as positive training samples with the help of object count constraints so that the detector will learn the appearance of a single cat.

We formulate the problem as a region selection problem. Given a set of boxes $\mathbf{B} = \{b_1, \dots, b_N\}$ and the corresponding confidence scores $\mathbf{P} = \{p_1, \dots, p_N\}$ (the confidence score can be the detection score of a region in each detector refinement iteration), a subset \mathbf{G} is selected as the set of positive training regions where $|\mathbf{G}| = C$ and C indicates the per-class object count. We identify a good subset \mathbf{G} using a greedy algorithm applied to a graphical representation of the set of boxes. Each box is represented as a node in the graph, and two nodes are connected if the spatial overlap of their corresponding boxes is below a threshold (See Fig. 2). The greedy algorithm provides an approximation to the following optimization problem:

$$\begin{aligned} \mathbf{G}^* &= \arg \max_{\mathbf{G}} \sum_{b_k \in \mathbf{G}} p_k, \\ \text{s.t. } |\mathbf{G}| &= C, a_o(b_i, b_j) < T \forall b_i, b_j \in \mathbf{G}, i \neq j. \end{aligned} \quad (1)$$

To encourage selecting regions containing just one object, we use the asymmetric area of overlap, *i.e.*, $a_o(b_i, b_j) = \frac{\text{area}(b_i \cap b_j)}{\text{area}(b_j)}$, which has been proposed in [7, 8] to model a spatial overlap between two boxes, where b_i is a box previously selected by the greedy algorithm and b_j indicates a box to be considered for selection. T is the overlap threshold. If the algorithm has previously added a large box to the solution, thresholding on a_o will discourage the selection of its subregions, regardless of their sizes.¹ So, to deliver a high total score, the algorithm prefers C small high-scoring boxes to one large box, even though the large box may have the highest score.

We conduct region selection only after applying non-maximum suppression on a complete set of the detection boxes, so the number of nodes is limited to a reasonable

number, and the computation cost is low in practice. The algorithm is summarized in Alg. 1.

Algorithm 1: Count-based Region Selection (CRS)

Input : $\mathbf{B} = \{b_1, \dots, b_N\}$, $\mathbf{P} = \{p_1, \dots, p_N\}$, T , C ;
 \mathbf{B} is a list of candidate boxes;
 \mathbf{P} is the corresponding scores;
 T is the overlap threshold;
 C indicates the object count;

Initialization: Sort (descend) \mathbf{B} based on \mathbf{P} ;

$\mathbf{G}^* \leftarrow \emptyset$; $s_{max} \leftarrow 0$;

Output: \mathbf{G}^*

```

for  $i \in \{1, \dots, N\}$  do
   $\mathbf{G} \leftarrow b_i$ ;  $s \leftarrow p_i$ ;
  for  $j \in \{i + 1, \dots, N\}$  do
    if  $a_o(b_i, b_j) < T (\forall b_k \in \mathbf{G})$  then
       $\mathbf{G} \leftarrow \mathbf{G} \cup \{b_j\}$ ;  $s \leftarrow s + p_j$ 
      if  $|\mathbf{G}| == C$  or  $j == N$  then
        if  $s > s_{max}$  then
           $s_{max} \leftarrow s$ ;  $\mathbf{G}^* \leftarrow \mathbf{G}$ 
        break;

```

3.2. Detector Refinement Structures with CRS

3.2.1 Alternating Detector Refinement (ADR)

We first integrate CRS into an alternating WSL refinement architecture, where a poor weakly supervised detector can be refined iteratively. The architecture is shown in Fig. 3, where a WSL detector alternates between generating high-quality regions as pseudo ground-truth (GT) boxes and refining itself using these GT boxes. Some WSL methods are based on a strategy like this [3, 13]. The major difference is that we use CRS to select high-quality positive regions as the GT boxes to refine a detector.

Initialization phase. We first generate a set of box candidates from the training data using a pre-trained WSL detector. This set of box candidates is treated as the initialized pseudo GTs and will be refined iteratively afterwards.

Alternating training phase. We use Fast R-CNN [12] as our WSL network. Starting from the initialized pseudo GT boxes, Fast R-CNN alternates between improving itself via retraining with the pseudo GT boxes generated by CRS and generating a refined set of GT candidate boxes on the training images. Since Fast R-CNN is trained using pseudo GT boxes, it does not have access to any true bounding box supervision during the training process. So, it is still a WSL detector.

3.2.2 Online Detector Refinement (ODR)

As argued in [29], the alternating strategy has two potential limitations: 1) it is time consuming to alternate between

¹The commonly used symmetric intersection-over-union measure would allow sufficiently small regions even if they were fully overlapped by an existing large box.

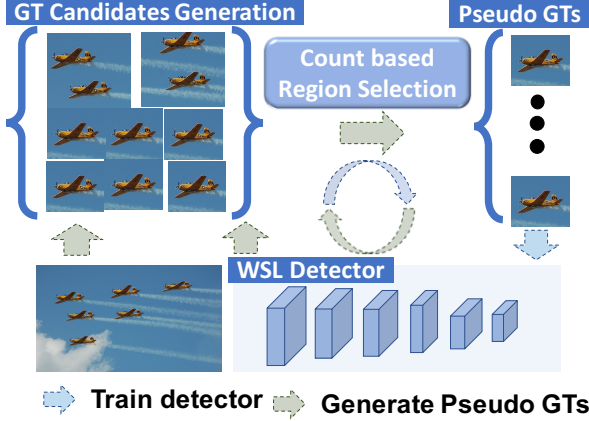


Figure 3. Alternating detector refinement. Count-based Region Selection (CRS) is applied to select high-quality positive training regions from the ground-truth (GT) candidate boxes generated by a WSL detector. The WSL detector is then refined using these high-quality regions. The GT generation and detector refinement are conducted in alternating fashion to progressively improve the detector.

training on the fixed labels and generating labels by the trained model; 2) separating refinements into different iterations might harm the performance since it hinders the procedure from sharing image representations across iterations.

Based on [29], we propose an online detector refinement framework integrated with CRS. An illustration of the proposed method is shown in Fig. 4. A Multiple Instance Detection Network (MIDN) and several detector refinement stages share the same feature representation extracted from a backbone structure (VGG16 [27] in our case). The MIDN utilizes an object-category label to supervise its training as in [29, 1]. Each detector refinement network outputs the classification score and predicted bounding box for each region proposal. Compared to [29], we have two major differences: 1) we use CRS to generate high-quality regions as pseudo GTs rather than just choosing the top-scoring region; 2) we use both classification loss and bounding box regression loss for detector refinement, just as RCNNs do.

4. Experiments

4.1. Experimental Setup

Datasets and Evaluate Metrics. Experiments are conducted on Pascal VOC2007 [10] and VOC2012 [11] which contain 20 object categories. For VOC2007, all models are trained on *trainval* set which contains 5,011 images and evaluated on *test* set which includes 4,952 images. For VOC2012, models are trained on 5,717 images of *train* set and evaluated on 5,823 images in the *val* set.

We use two widely used metrics to do evaluation, Correct localization (CorLoc) [20] and Average Precision (AP) [9].

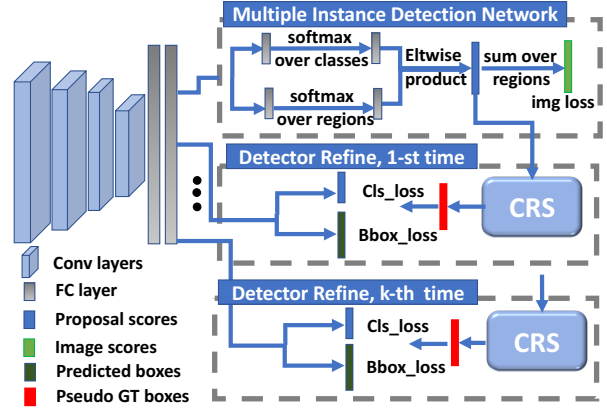


Figure 4. Online detector refinement with CRS. Feature representations of region proposals are extracted by convolutional neural networks followed by 2 fully-connected layers. The Multiple Instance Detection Network [29, 1] and multiple detector networks share the same feature representation to refine the detector at all stages together. *Cls_loss* indicates the classification loss and *Bbox_loss* indicates bounding box regression loss.

CorLoc evaluates localization accuracy by measuring if the maximum response point of a detection is inside the ground truth bounding box. AP evaluates models by comparing IoU between output and ground truth bounding boxes.

Implementation Details. In CRS, the only parameter is the overlap threshold, T . We set $T = 0.1$ and fix it for all models at all the iterations on both datasets.

Following [13, 29], we set the total iteration number to 3 and use VGG16 [27] as the backbone structure for both ADR and ODR. For fair comparison, all reported results of CNN-based state-of-the-art methods also use VGG16. In ADR, we strictly follow the steps of training Fast-RCNN at each iteration and use all the released default training parameters² except that we use the generated pseudo GT boxes instead of the bounding box labels. In ODR, we follow basic MIDN structure and training process in [29], and use the parameters released by the author.³ Note that we use the same classification and bounding box regression loss in ODR as in [12].

4.2. Variants of Our Approach

To demonstrate the effectiveness of C-WSL, we investigate several variants of our frameworks:

C-WSL: WSLPDA/OICR+ADR indicates ADR initialized with a pre-trained WSLPDA [17] (or OICR [29]) model where CRS is used to select confident GT boxes in each iteration. Then, a Fast-RCNN is alternatively refined as we mentioned in Sec. 3.2.1.

²<https://github.com/rbgirshick/fast-rcnn>

³<https://github.com/ppengtang/oicr>

Methods	areo	bike	bird	boat	bottle	bus	car	cat	chair	cow	table	dog	horse	mbike	person	plant	sheep	sofa	train	tv	mAP
Cinbis et al. [3]	39.3	43.0	28.8	20.4	8.0	45.5	47.9	22.1	8.4	33.5	23.6	29.2	38.5	47.9	20.3	20.0	35.8	30.8	41.0	20.1	30.2
Wang et al. [30]	48.8	41.0	23.6	12.1	11.1	42.7	40.9	35.5	11.1	36.6	18.4	35.3	34.8	51.3	17.2	17.4	26.8	32.8	35.1	45.6	30.9
Jie et al. [13]	52.2	47.1	35.0	26.7	15.4	61.3	66.0	54.3	3.0	53.6	24.7	43.6	48.4	65.8	6.6	18.8	51.9	43.6	53.6	62.4	41.7
WSDDN [1]	39.4	50.1	31.5	16.3	12.6	64.5	42.8	42.6	10.1	35.7	24.9	38.2	34.4	55.6	9.4	14.7	30.2	40.7	54.7	46.9	34.8
WSDDN+Context [14]	57.1	52.0	31.5	7.6	11.5	55.0	53.1	34.1	1.7	33.1	49.2	42.0	47.3	56.6	15.3	12.8	24.8	48.9	44.4	47.8	36.3
WSDDN-Ens. [1]	46.4	58.3	35.5	25.9	14.0	66.7	53.0	39.2	8.9	41.8	26.6	38.6	44.7	59.0	10.8	17.3	40.7	49.6	56.9	50.8	39.3
WCCN-3stage [5]	49.5	60.6	38.6	29.2	16.2	70.8	56.9	42.5	10.9	44.1	29.9	42.2	47.9	64.1	13.8	23.5	45.9	54.1	60.8	54.5	42.8
WSLPDA [17]	54.5	47.4	41.3	20.8	17.7	51.9	63.5	46.1	21.8	57.1	22.1	34.4	50.5	61.8	16.2	29.9	40.7	15.9	55.3	40.2	39.5
OICR [29]	58.0	62.4	31.1	19.4	13.0	65.1	62.2	28.4	24.8	44.7	30.6	25.3	37.8	65.5	15.7	24.1	41.7	46.9	64.3	62.6	41.2
OICR-Ens.+FRCNN [29]	64.5	64.4	44.1	25.9	16.9	67.8	68.4	33.2	9.0	57.5	46.4	21.7	57.8	64.3	10.0	23.7	50.6	60.9	64.7	58.0	45.5
C-WSL:ODR	62.7	63.7	40.0	25.5	17.7	70.1	68.3	38.9	25.4	54.5	41.6	29.9	37.9	64.2	11.3	27.4	49.3	54.7	61.4	67.4	45.6
C-WSL:ODR+FRCNN	61.9	61.9	48.6	28.7	23.3	71.1	71.3	38.7	28.5	60.6	45.4	26.3	49.7	65.5	7.2	27.3	54.7	61.6	63.2	59.5	47.8

Table 1. Comparison with the state-of-the-art in terms of mAP on the VOC2007 test set. Our number is marked in **red** (**blue**) if it is the best (second best) in the column. The numbers of OICR-Ens.+FRCNN are reproduced by using the code released by the author. Our variants are in **bold**.

Methods	areo	bike	bird	boat	bottle	bus	car	cat	chair	cow	table	dog	horse	mbike	person	plant	sheep	sofa	train	tv	Avg.
Cinbis et al. [3]	65.3	55.0	52.4	48.3	18.2	66.4	77.8	35.6	26.5	67.0	46.9	48.4	70.5	69.1	35.2	35.2	69.6	43.4	64.6	43.7	52.0
Wang et al. [30]	80.1	63.9	51.5	14.9	21.0	55.7	74.2	43.5	26.2	53.4	16.3	56.7	58.3	69.5	14.1	38.3	58.8	47.2	49.1	60.9	48.5
Jie et al. [13]	72.7	55.3	53.0	27.8	35.2	68.6	81.9	60.7	11.6	71.6	29.7	54.3	64.3	88.2	22.2	53.7	72.2	52.6	68.9	75.5	56.1
WSDDN [1]	65.1	58.8	58.5	33.1	39.8	68.3	60.2	59.6	34.8	64.5	30.5	43.0	56.8	82.4	25.5	41.6	61.5	55.9	65.9	63.7	53.5
WSDDN+Context [14]	83.3	68.6	54.7	23.4	18.3	73.6	74.1	54.1	8.6	65.1	47.1	59.5	67.0	83.5	35.3	39.9	67.0	49.7	63.5	65.2	55.1
WSDDN-Ens. [1]	68.9	68.7	65.2	42.5	40.6	72.6	75.2	53.7	29.7	68.1	33.5	45.6	65.9	86.1	27.5	44.9	76.0	62.4	66.3	66.8	58.0
WCCN-3stage [5]	83.9	72.8	64.5	44.1	40.1	65.7	82.5	58.9	33.7	72.5	25.6	53.7	67.4	77.4	26.8	49.1	68.1	27.9	64.5	55.7	56.7
SP-VGGNet [31]	85.3	64.2	67.0	42.0	16.4	71.0	64.7	88.7	20.7	63.8	58.0	84.1	84.7	80.0	60.0	29.4	56.3	68.1	77.4	30.5	60.6
WSLPDA [17]	78.2	67.1	61.8	38.1	36.1	61.8	78.8	55.2	28.5	68.8	18.5	49.2	64.1	73.5	21.4	47.4	64.6	22.3	60.9	52.3	52.4
OICR [29]	81.7	80.4	48.7	49.5	32.8	81.7	85.4	40.1	40.6	79.5	35.7	33.7	60.5	88.8	21.8	57.9	76.3	59.9	75.3	81.4	60.6
OICR-Ens.+FRCNN [29]	88.3	78.8	62.8	48.9	38.9	83.2	85.4	50.0	21.9	77.4	45.6	41.9	79.3	91.6	12.6	60.8	86.6	70.2	80.2	79.9	64.2
C-WSL:ODR	86.3	80.4	58.3	50.0	36.6	85.8	86.2	47.1	42.7	81.5	42.2	42.6	50.7	90.0	14.3	61.9	85.6	64.2	77.2	82.4	63.3
C-WSL:ODR+FRCNN	85.8	78.0	61.6	52.1	44.7	81.7	88.4	49.1	50.0	82.9	44.1	44.4	63.9	92.4	14.3	60.4	86.6	68.3	80.6	82.8	65.6

Table 2. Comparison with the state-of-the-art in terms of CorLoc (%) on the VOC2007 trainval set. Our number is marked in **red** (**blue**) if it is the best (second best) in the column. The numbers of OICR-Ens.+FRCNN are reproduced by using the code released by the author. Our variants are in **bold**.

C-WSL:ODR indicates the structure shown in Fig. 4.

C-WSL:ODR+FRCNN. Inspired by [17, 29], we use the top-scoring region generated by **C-WSL:ODR** to train a separate Fast RCNN to improve results.

4.3. Comparison with State-of-the-art Approaches

Comparison in terms of *mAP* on VOC2007 *test* set and *CorLoc* on VOC2007 *trainval* set are shown in Tab. 1 and 2, respectively. Overall, the proposed **C-WSL:ODR+FRCNN** outperforms all the existing state-of-the-art methods using both *CorLoc* and *mAP* measurements.

Tab. 3 and 4 compare our variants with the two baseline detectors, *i.e.*, WSLPDA [17] and OICR [29]. The results suggest that even the simple ADR strategy can significantly improve the results. Moreover, if we use object count information, we can largely improve WSLPDA by 6.2% *mAP* (9.5% average *CorLoc*) and OICR by 5.2% *mAP* (4.0% average *CorLoc*). **C-WSL** improves the results of WSLPDA+ADR on 17 (15) out of 20 categories and the results of OICR+ADR on 10 (10) out of 20 categories in terms of *mAP* on VOC2007 *test* set (in terms of *CorLoc* on VOC2007 *trainval* set).

As stated in Sec. 1, the object count information is helpful to avoid a detector localizing on multiple objects. To

demonstrate this point, we first calculate the percentage of images that have more than one per-class object (multi-objects percentage) in the VOC2007 *test* set. As shown in Fig. 5, “bottle”, “car”, “chair”, “cow”, “person”, “plant” and “sheep” have a high percentage of images which include more than one object in the corresponding category. As shown in Tab. 1 and 2, **C-WSL:ODR+FRCNN** outperforms other methods for 5 out of these 7 categories. When looking into the effect of the object count supervision on WSLPDA and OICR, we see significant improvement on these categories as shown in Tab. 3 and 4. Consider the “sheep” category for example. **C-WSL:WSLPDA+ADR** improves WSLPDA+ADR by 13.4% *CorLoc* and 10.4% *AP*. **C-WSL:OICR+ADR** improves OICR+ADR by 3.1% *CorLoc* and 6.1% *AP*. Fig. 8 shows some examples of training regions selected by OICR+CRS and OICR. OICR tends to select regions containing multiple instances, while object count helps to obtain regions including a single instance. Qualitative comparison between our **C-WSL:ODR+FRCNN** and OICR-Ens.+FRCNN on VOC2007 *test* set is shown in Fig. 9, demonstrating that our approach achieves more precise localization when multiple per-class objects appear in an image. We will further analyze our approach on images with different number of objects in Sec. 4.4.

Methods	areo	bike	bird	boat	bottle	bus	car	cat	chair	cow	table	dog	horse	mbike	person	plant	sheep	sofa	train	tv	mAP
WSLPDA [17]	54.5	47.4	41.3	20.8	17.7	51.9	63.5	46.1	21.8	57.1	22.1	34.4	50.5	61.8	16.2	29.9	40.7	15.9	55.3	40.2	39.5
WSLPDA+ADR	57.9	68.3	47.8	20.3	12.2	52.9	67.6	68.8	24.6	50.0	24.9	49.8	54.8	63.5	14.1	27.4	41.2	19.5	57.1	30.7	42.7
C-WSL:WSLPDA+ADR	60.5	70.1	52.5	24.7	24.4	63.6	71.8	58.1	26.0	66.4	26.5	34.7	55.0	65.8	8.8	31.9	51.6	20.4	60.0	41.8	45.7
OICR [29]	58.0	62.4	31.1	19.4	13.0	65.1	62.2	28.4	24.8	44.7	30.6	25.3	37.8	65.5	15.7	24.1	41.7	46.9	64.3	62.6	41.2
OICR+ADR	58.1	61.2	43.3	24.4	19.4	65.5	67.1	34.3	3.6	56.5	45.5	26.4	61.9	60.7	10.4	23.6	49.2	62.1	61.4	64.2	44.9
C-WSL:OICR+ADR	61.7	66.8	45.6	21.1	23.5	67.2	73.8	32.5	10.6	54.6	42.9	16.6	59.2	63.3	11.0	25.4	55.3	61.3	67.4	67.8	46.4

Table 3. Comparison with baseline detectors, *i.e.*, WSLPDA and OICR in terms of mAP on the VOC2007 test set. The table contains two comparison groups which are separated by double solid lines. Each group shows how much ADR improve a baseline detector and C-WSL increase the result. Underline is used if C-WSL gives the best result in the group for the category. Our variants are in **bold**

Methods	areo	bike	bird	boat	bottle	bus	car	cat	chair	cow	table	dog	horse	mbike	person	plant	sheep	sofa	train	tv	Avg.
WSLPDA [17]	78.2	67.1	61.8	38.1	36.1	61.8	78.8	55.2	28.5	68.8	18.5	49.2	64.1	73.5	21.4	47.4	64.6	22.3	60.9	52.3	52.4
WSLPDA+ADR	84.6	76.9	69.7	41.0	21.8	68.5	83.2	77.6	34.4	76.7	19.8	73.7	75.2	84.7	26.3	53.8	70.1	22.3	73.8	50.9	59.2
C-WSL:WSLPDA+ADR	83.3	80.0	70.9	51.6	41.2	73.6	85.3	67.7	40.7	79.5	20.9	54.7	79.6	87.1	24.5	56.8	83.5	20.7	76.0	60.2	61.9
OICR [29]	81.7	80.4	48.7	49.5	32.8	81.7	85.4	40.1	40.6	79.5	35.7	33.7	60.5	88.8	21.8	57.9	76.3	59.9	75.3	81.4	60.6
OICR+ADR	85.8	76.9	65.8	49.5	38.5	83.2	84.8	49.7	14.0	79.5	46.8	41.2	80.3	89.2	15.0	60.1	84.5	66.4	78.3	80.6	63.5
C-WSL:OICR+ADR	85.4	78.0	65.5	49.5	43.5	84.3	87.5	48.0	23.6	80.8	43.3	38.8	79.9	92.8	15.8	60.1	87.6	66.4	81.0	80.3	64.6

Table 4. Comparison with the baseline detectors, *i.e.*, WSLPDA and OICR in terms of CorLoc (%) on the VOC2007 trainval set. The table contains two comparison groups which are separated by double solid lines. Each group shows how much ADR improve a baseline detector and C-WSL increase the result. Underline is used if C-WSL gives the best result in the group for the category. Our variants are in **bold**

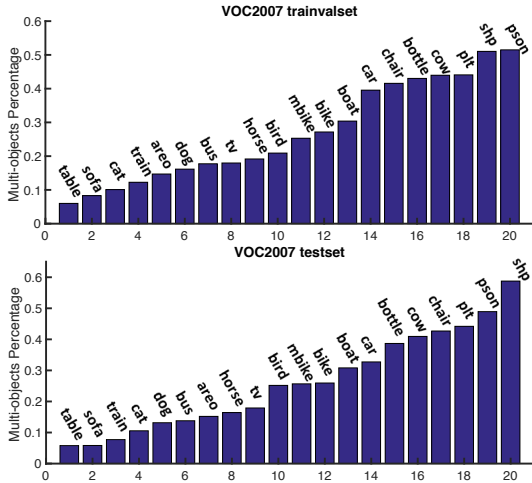


Figure 5. Image number of multiple-objects over image number of non-zero objects. Note that “pson” means “person”, “plt” means “plant” and “shp” denotes “sheep”. C-WSL works better on most classes with high multiple-objects percentage. See Sec. 4.3.

Tab. 5 and 6 show the comparison of C-WSL with the state-of-the-art on VOC2012. Note that results of WSLPDA and OICR models are reproduced by running the pre-trained model and the code released by the authors. The results suggest that our method outperforms the state-of-the-art method (*OICR-Ens.+FRCNN*) by 2.6% in *mAP* on VOC2012 *val* set and by 2.8% in *CorLoc* on VOC2012 *train* set. C-WSL improves the results of *WSLPDA+ADR* on 12 (10) out of 20 categories and the results of *OICR+ADR* on 10 (12) out of 20 categories in terms of *mAP* on VOC2012 *val* set (in terms of *CorLoc* on VOC2012 *train* set).

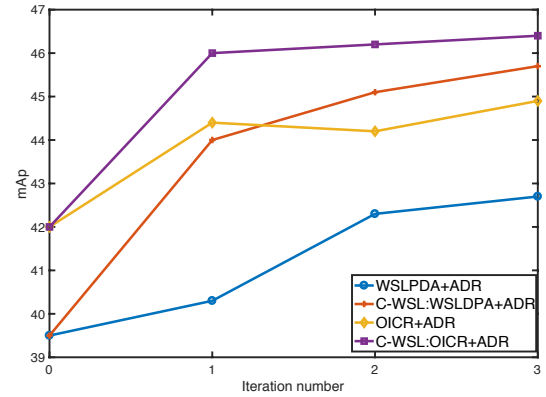


Figure 6. Improvement of each model as the number of ADR iteration increases on VOC2007 *test* set. C-WSL approaches improves faster than others.

4.4. Ablation Analysis

Two major components contribute to the success of our approach. One is the iterative training process (alternating/online) and the other one is the per-class object count supervision. In Tab. 3 and 4, we can see the improvement by adding ADR and object count into the system. For WSLPDA [17], iterative training (ADR) improves *mAP* by 3.2% and the count information (CRS) increase it by 3%. For OICR [29], ADR helps by increasing 3.7% *mAP* and CRS contributes 1.5%. In the following, we analyze each components in detail.

Number of iterations. ADR performance as a function of the number of iterations using the WSLPDA and OICR models is shown in Fig. 6. Generally, models improve as the number of iterations increases. Especially when adding object count supervision into the framework, the results of

Methods	areo	bike	bird	boat	bottle	bus	car	cat	chair	cow	table	dog	horse	mbike	person	plant	sheep	sofa	train	tv	mAP
Jie <i>et al.</i> [13]	60.9	53.3	31.0	16.4	18.2	58.2	50.5	55.6	9.1	42.1	12.1	43.4	45.3	64.6	7.4	19.3	44.8	39.3	51.4	57.2	39.0
OICR-Ens.+FRCNN [29]	71.0	68.2	52.7	20.1	27.2	57.3	57.1	19.0	8.0	50.6	30.2	34.5	63.3	69.5	1.2	20.5	48.5	55.2	41.1	60.4	42.8
WSLPDA [17]	42.2	27.8	32.7	4.2	13.7	52.1	35.8	48.3	11.8	31.7	4.9	30.4	45.3	51.8	11.5	13.4	33.5	7.2	45.6	38.4	29.1
WSLPDA+ADR	70.0	65.6	46.3	14.4	22.8	57.5	54.2	67.5	16.1	45.0	4.4	40.0	51.7	71.8	5.8	27.7	38.3	11.7	55.2	34.1	40.0
C-WSL:WSLPDA+ADR	69.8	62.8	52.7	16.7	28.3	61.1	56.6	58.0	18.5	47.8	5.1	36.3	53.3	66.8	6.8	24.2	47.1	11.0	60.1	43.4	41.3
OICR [29]	71.0	59.1	42.3	27.4	20.2	58.7	46.4	18.6	18.1	45.7	21.7	20.5	53.1	68.5	1.8	15.7	42.7	40.0	41.0	61.5	38.7
OICR+ADR	67.0	63.1	50.8	12.8	23.8	55.3	55.1	16.1	5.2	47.2	23.4	28.2	55.9	69.2	1.9	21.5	46.5	49.9	35.9	63.8	39.6
C-WSL:OICR+ADR	71.3	68.3	50.9	17.1	24.8	60.9	56.4	13.9	14.5	54.6	22.2	25.7	57.7	70.4	1.6	20.0	55.8	46.0	35.7	62.9	41.5
C-WSL:ODR	74.0	67.3	45.6	29.2	26.8	62.5	54.8	21.5	22.6	50.6	24.7	25.6	57.4	71.0	2.4	22.8	44.5	44.2	45.2	66.9	43.0
C-WSL:ODR+FRCNN	75.3	71.6	52.6	32.5	29.9	62.9	56.9	16.9	24.5	59.0	28.9	27.6	65.4	72.6	1.4	23.0	49.4	52.3	42.4	62.2	45.4

Table 5. Comparison with the state-of-the-art in terms of mAP on the VOC2012 *val* set. Our number is marked in **red** if it is the best in the column. Refer to Tab. 3 and 4 for the meaning of underline. Our variants are in **bold**

Methods	areo	bike	bird	boat	bottle	bus	car	cat	chair	cow	table	dog	horse	mbike	person	plant	sheep	sofa	train	tv	Avg.
OICR-Ens.+FRCNN [29]	85.4	81.5	70.4	44.7	46.6	83.6	78.4	33.9	29.3	83.2	51.6	50.5	86.1	88.0	11.0	56.7	82.5	69.1	65.1	83.6	64.1
WSLPDA [17]	80.5	63.7	64.4	34.1	29.3	76.7	71.5	62.8	30.3	76.1	23.0	55.3	75.2	77.7	18.7	56.4	66.7	25.1	66.5	54.8	55.4
WSLPDA+ADR	87.2	79.7	72.4	38.6	40.9	82.6	75.2	79.8	35.1	81.3	18.9	62.1	82.4	83.9	21.6	60.9	75.4	29.5	74.5	55.5	61.9
C-WSL:WSLPDA+ADR	85.7	77.2	73.4	38.6	46.4	84.9	75.8	69.1	43.0	76.8	20.1	58.6	79.8	79.6	20.3	57.8	79.5	35.4	76.4	61.9	62.0
OICR [29]	86.6	80.4	65.2	57.6	42.1	85.4	72.5	28.0	45.7	79.4	46.2	34.0	78.2	87.2	7.5	55.0	83.6	58.5	62.2	84.3	62.0
OICR+ADR	84.5	79.0	72.4	39.0	47.1	83.6	79.9	31.9	25.0	84.5	48.7	48.3	87.8	88.7	13.3	55.0	82.5	67.4	65.1	83.9	63.4
C-WSL:OICR+ADR	86.6	80.8	73.9	43.2	44.4	87.7	76.2	32.2	34.0	87.1	49.1	46.2	88.2	91.2	12.1	57.1	78.4	65.5	65.1	85.3	64.2
C-WSL:ODR	90.9	81.1	64.9	57.6	50.6	84.9	78.1	29.8	49.7	83.9	50.9	42.6	78.6	87.6	10.4	58.1	85.4	61.0	64.7	86.6	64.9
C-WSL:ODR+FRCNN	92.1	84.3	69.9	58.3	53.9	86.8	80.4	30.6	52.6	83.9	54.7	45.8	83.2	90.1	12.7	56.4	86.0	64.9	66.5	84.3	66.9

Table 6. Comparison with the state-of-the-art in terms of *CorLoc* on the VOC2012 *train* set. Our number is marked in **red** if it is the best in the column. Refer to Tab. 3 and 4 for the meaning of underline. Our variants are in **bold**

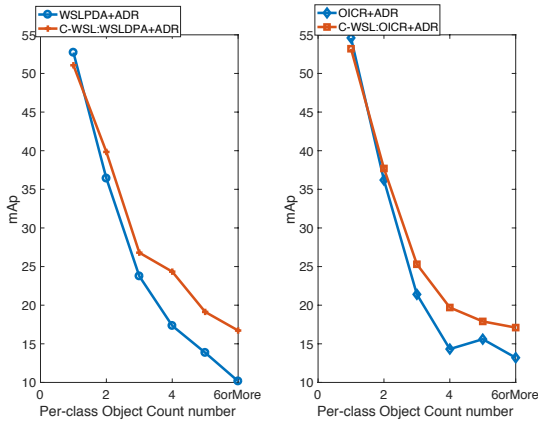


Figure 7. Evaluation on images with different per-class object counts on VOC2007. WSL detectors with poor bounding box prediction make more mistakes when there are more instances in a test image; our approach is able to select tight boxes around objects and outperforms in the presence of multiple instances.

both WSLDPA and OICR models improve faster, which demonstrates the advantage of count information in WSL.

Number of object instances per image. Adding the object count constraint in the training process helps a detector focus on a single object rather than multiple objects. To demonstrate this, we partition images in the VOC2007 *test* set based on their per-class object count and re-evaluate our approaches on each subset.

The evaluation results is shown in Fig. 7. For both WSLPDA and OICR, the performance is much better under C-WSL. Mostly, the gaps between curves of with and with-

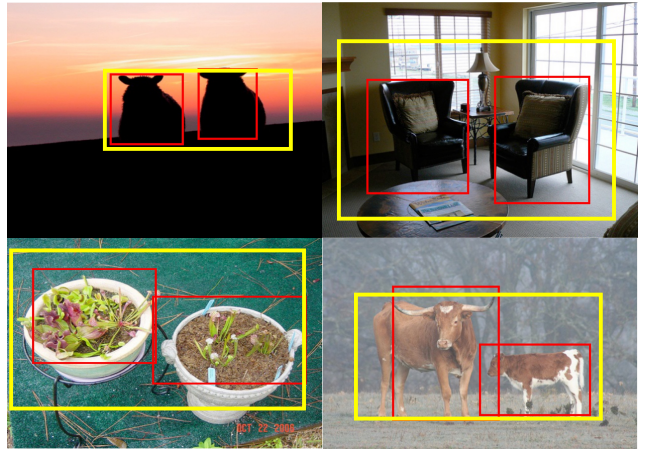


Figure 8. Examples of the training regions selected by *OICR+CRS* (red) and *OICR* (yellow). The top-scoring boxes selected by *OICR* contain multiple object instances. While, object count information helps to select regions, each covering a single instance.

out C-WSL are bigger as the object instance count number increases.

4.5. Error Analysis

We now analyze some failure cases. The results shown in Tab. 1, 2, 5 and 6 suggest that most existing WSL detectors perform poorly on the “person” category: in the strongly supervised setting, detectors can achieve more than 76% mAP on the VOC2007 *test* set (e.g. 76.6% [19] and 76.3% [25]), while the best WSL detection result on “person” is 20.3% (see Tab. 1). This result is likely due to the large appearance

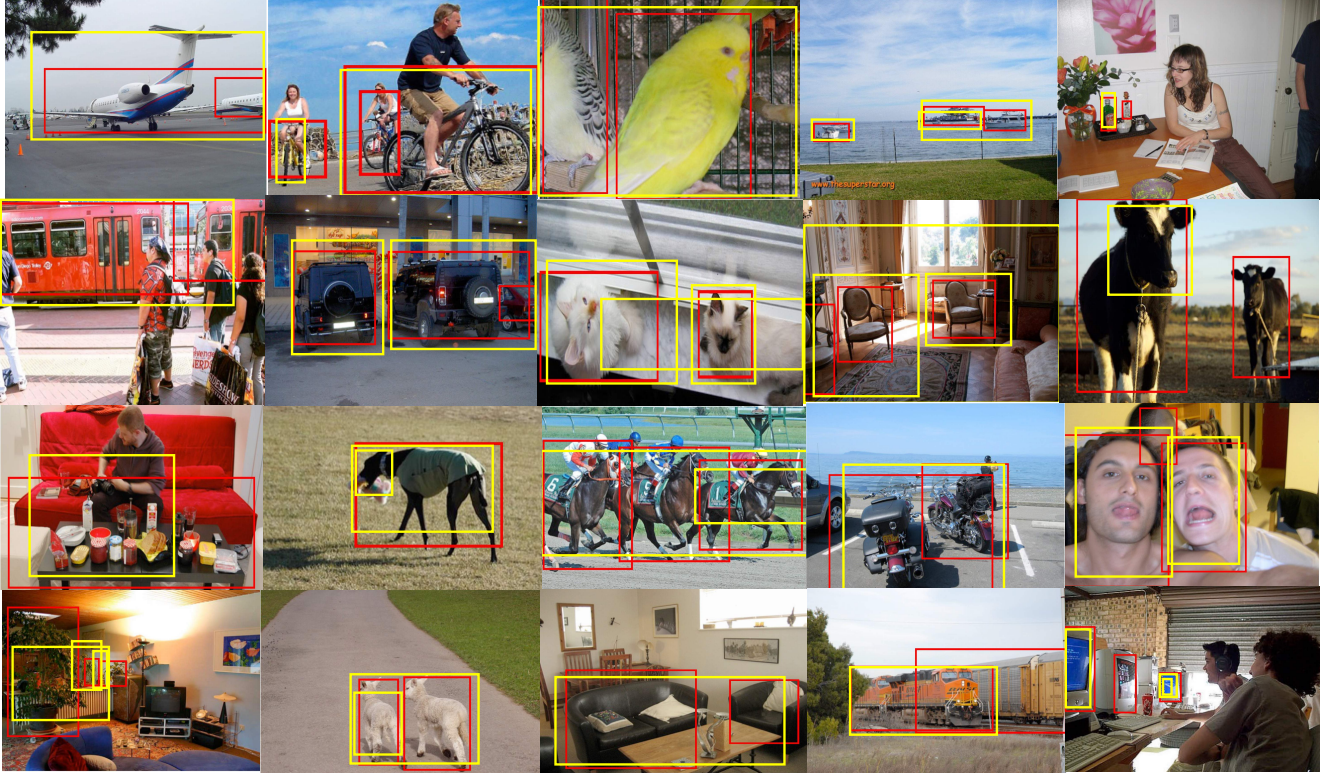


Figure 9. Qualitative comparison between our *CWSL:ODR+FRCNN* (red boxes) and *OICR+FRCNN* (yellow boxes) on the VOC2007 *test* set over the 20 classes. Our detector detects much tighter bounding boxes, yields much fewer boxes with multiple objects in them, and finds instances more accurately.



Figure 10. Some examples of the common failure cases of our approach (*CWSL:ODR+FRCNN*) on the “person” category of VOC2007 *test* set.

variations of persons in the dataset. Without constraints provided by tight bounding boxes, rigid parts are easier to learn and mostly sufficient to differentiate the object from others. Consequently, WSL detectors focus on local parts instead of the whole object as shown in Fig. 10.

Intuitively, this could be overcome if we had even rough estimates of the size of object instances. We conducted a preliminary experiment as follows. Suppose that we know

the size of the smallest instance of an object category in an image and we assume all the object parts are smaller than the smallest object. This assumption is not generally true and we use it just as a proof-of-concept. We preprocess the region candidates by removing all boxes whose size is smaller than the smallest object and then conduct *CWSL:WSLPDA+ADR*. The *AP* on “person” improves to 40.0% (from 8.8%) and the *mAP* over all the classes improves to 52.7% (from 45.7%).

5. Conclusions

We proposed a Count-guided Weakly Supervised Localization (*CWSL*) framework where a cheap and effective form of image-level supervision, *i.e.*, per-class object count is used to select training regions each of which tightly covers a single object instance for detector refinement. As a part of *CWSL*, we proposed a Count-based Region Selection (*CRS*) algorithm to perform high-quality region selection. Also, we integrated *CRS* into two detector refinement architectures to improve WSL detectors. Experimental results demonstrate the effectiveness of *CWSL*.

References

- [1] H. Bilen and A. Vedaldi. Weakly supervised deep detection networks. In *The IEEE Conference on Computer Vision and Pattern Recognition (CVPR)*, June 2016.
- [2] P. Chattopadhyay, R. Vedantam, R. RS, D. Batra, and D. Parikh. Counting everyday objects in everyday scenes. *arXiv preprint arXiv:1604.03505*, 2016.
- [3] R. G. Cinbis, J. Verbeek, and C. Schmid. Weakly supervised object localization with multi-fold multiple instance learning. *IEEE transactions on pattern analysis and machine intelligence*, 39(1):189–203, 2017.
- [4] D. H. Clements. Subitizing: What is it? why teach it? *Teaching children mathematics*, 5(7):400, 1999.
- [5] A. Diba, V. Sharma, A. Pazandeh, H. Pirsiavash, and L. Van Gool. Weakly supervised cascaded convolutional networks. *arXiv preprint arXiv:1611.08258*, 2016.
- [6] T. G. Dietterich, R. H. Lathrop, and T. Lozano-Pérez. Solving the multiple instance problem with axis-parallel rectangles. *Artificial intelligence*, 89(1):31–71, 1997.
- [7] P. Dollár, Z. Tu, P. Perona, and S. Belongie. Integral channel features. 2009.
- [8] P. Dollar, C. Wojek, B. Schiele, and P. Perona. Pedestrian detection: An evaluation of the state of the art. *IEEE transactions on pattern analysis and machine intelligence*, 34(4):743–761, 2012.
- [9] M. Everingham, L. Van Gool, C. K. Williams, J. Winn, and A. Zisserman. The pascal visual object classes (voc) challenge. *International journal of computer vision*, 88(2):303–338, 2010.
- [10] M. Everingham, L. Van Gool, C. K. I. Williams, J. Winn, and A. Zisserman. The PASCAL Visual Object Classes Challenge 2007 (VOC2007) Results. <http://www.pascal-network.org/challenges/VOC/voc2007/workshop/index.html>.
- [11] M. Everingham, L. Van Gool, C. K. I. Williams, J. Winn, and A. Zisserman. The PASCAL Visual Object Classes Challenge 2012 (VOC2012) Results. <http://www.pascal-network.org/challenges/VOC/voc2012/workshop/index.html>.
- [12] R. Girshick. Fast r-cnn. In *Proceedings of the IEEE International Conference on Computer Vision*, pages 1440–1448, 2015.
- [13] Z. Jie, Y. Wei, X. Jin, J. Feng, and W. Liu. Deep self-taught learning for weakly supervised object localization. *arXiv preprint arXiv:1704.05188*, 2017.
- [14] V. Kantorov, M. Oquab, M. Cho, and I. Laptev. Context-locnet: Context-aware deep network models for weakly supervised localization. In *European Conference on Computer Vision*, pages 350–365. Springer, 2016.
- [15] D. Kim, D. Yoo, I. S. Kweon, et al. Two-phase learning for weakly supervised object localization. *arXiv preprint arXiv:1708.02108*, 2017.
- [16] A. Kolesnikov and C. H. Lampert. Improving weakly-supervised object localization by micro-annotation. *arXiv preprint arXiv:1605.05538*, 2016.
- [17] D. Li, J.-B. Huang, Y. Li, S. Wang, and M.-H. Yang. Weakly supervised object localization with progressive domain adaptation. In *The IEEE Conference on Computer Vision and Pattern Recognition (CVPR)*, June 2016.
- [18] T.-Y. Lin, M. Maire, S. Belongie, J. Hays, P. Perona, D. Ramanan, P. Dollár, and C. L. Zitnick. Microsoft coco: Common objects in context. In *European conference on computer vision*, pages 740–755. Springer, 2014.
- [19] W. Liu, D. Anguelov, D. Erhan, C. Szegedy, S. Reed, C.-Y. Fu, and A. C. Berg. SSD: Single shot multibox detector. In *ECCV*, 2016.
- [20] M. Oquab, L. Bottou, I. Laptev, and J. Sivic. Is object localization for free?-weakly-supervised learning with convolutional neural networks. In *Proceedings of the IEEE Conference on Computer Vision and Pattern Recognition*, pages 685–694, 2015.
- [21] D. P. Papadopoulos, J. R. Uijlings, F. Keller, and V. Ferrari. We don’t need no bounding-boxes: Training object class detectors using only human verification. In *Proceedings of the IEEE Conference on Computer Vision and Pattern Recognition*, pages 854–863, 2016.
- [22] D. P. Papadopoulos, J. R. Uijlings, F. Keller, and V. Ferrari. Training object class detectors with click supervision. *arXiv preprint arXiv:1704.06189*, 2017.
- [23] J. Redmon, S. Divvala, R. Girshick, and A. Farhadi. You only look once: Unified, real-time object detection. In *Proceedings of the IEEE Conference on Computer Vision and Pattern Recognition*, pages 779–788, 2016.
- [24] J. Redmon and A. Farhadi. Yolo9000: Better, faster, stronger. *arXiv preprint arXiv:1612.08242*, 2016.
- [25] S. Ren, K. He, R. Girshick, and J. Sun. Faster r-cnn: Towards real-time object detection with region proposal networks. In *Advances in neural information processing systems*, pages 91–99, 2015.
- [26] M. Shi, H. Caesar, and V. Ferrari. Weakly supervised object localization using things and stuff transfer. *arXiv preprint arXiv:1703.08000*, 2017.
- [27] K. Simonyan and A. Zisserman. Very deep convolutional networks for large-scale image recognition. *arXiv preprint arXiv:1409.1556*, 2014.
- [28] K. K. Singh and Y. J. Lee. Hide-and-seek: Forcing a network to be meticulous for weakly-supervised object and action localization. *arXiv preprint arXiv:1704.04232*, 2017.
- [29] P. Tang, X. Wang, X. Bai, and W. Liu. Multiple instance detection network with online instance classifier refinement. *arXiv preprint arXiv:1704.00138*, 2017.
- [30] C. Wang, W. Ren, K. Huang, and T. Tan. Weakly supervised object localization with latent category learning. In *European Conference on Computer Vision*, pages 431–445. Springer, 2014.
- [31] Y. Zhu, Y. Zhou, Q. Ye, Q. Qiu, and J. Jiao. Soft proposal networks for weakly supervised object localization. *arXiv preprint arXiv:1709.01829*, 2017.